Separation Science and Technology
Publication details, including instructions for authors and subscription information:
http://www.informaworld.com/smpp/title~content=t713708471

Recovery of Near-Anhydrous Ethanol as Gasoline Additive from Fermentation Products

Christos Boukouvalas[a]; Efi Markoulaki[a]; Kostis Magoulas[a]; Dimitrios Tassios[a]
[a] LABORATORY OF THERMODYNAMICS AND TRANSPORT PHENOMENA DEPARTMENT OF CHEMICAL ENGINEERING, NATIONAL TECHNICAL UNIVERSITY OF ATHENS, ATHENS, GREECE

To cite this Article Boukouvalas, Christos , Markoulaki, Efi , Magoulas, Kostis and Tassios, Dimitrios(1995) 'Recovery of Near-Anhydrous Ethanol as Gasoline Additive from Fermentation Products', Separation Science and Technology, 30: 11, 2315 — 2335

To link to this Article: DOI: 10.1080/01496399508013114

URL: http://dx.doi.org/10.1080/01496399508013114

SEPARATION SCIENCE AND TECHNOLOGY, 30(11), pp. 2315–2335, 1995

Recovery of Near-Anhydrous Ethanol as Gasoline Additive from Fermentation Products

CHRISTOS BOUKOUVALAS, EFI MARKOULAKI,
KOSTIS MAGOULAS, and DIMITRIOS TASSIOS
LABORATORY OF THERMODYNAMICS AND TRANSPORT PHENOMENA
DEPARTMENT OF CHEMICAL ENGINEERING
NATIONAL TECHNICAL UNIVERSITY OF ATHENS
9, HEROON POLYTECHNIOU STR., ZOGRAPHOU CAMPUS, 15773 ATHENS, GREECE

ABSTRACT

The use of near-anhydrous ethanol, obtained from fermentation products through low pressure distillation, as a gasoline additive is examined. To this purpose, a reliable model for predicting the azeotropic composition of an ethanol–water mixture as a function of the pressure is presented. It is developed by considering the available thermodynamic consistent experimental data and using the Wilson and the Virial equations for the liquid- and vapor-phase nonideality, respectively. It is concluded that, for an area with no extremely cold winters—minimum ambient temperature −20°C—alcohol with 96.5% (wt) purity can be used in a 90/10 (vol) gasohol mixture. Such an alcohol can be produced with a single distillation column operating at 140 mmHg pressure with an energy consumption of 5150 kJ/kg of product; or with a system of two columns with lower energy consumption but higher capital cost. These energy consumptions are very sensitive to the accuracy of the predicted azeotropic composition at the operating pressures.

INTRODUCTION

Use of near-anhydrous bioethanol as fuel has been examined in the last decades. Bioethanol can be used either as a fuel itself or as an additive to gasoline (gasohol). The former use has the advantage of permitting high water content in the fuel but a different engine design is required. The latter permits the use of fuel mixtures containing up to 10% bioethanol without any modifications of the engines, but has the disadvantage of possible phase splitting if the water concentration in the fuel exceeds rather small values. The water tolerance depends on the ambient temperature, the ethanol concentration, the aromatic content of the gasoline, and the presence of higher alcohols [Keller (1)].

Although many results on the recovery of ethanol from aqueous solutions with distillation have been presented in the literature [Black (2), Collura and Luyben (3)], great variation exists among their energy consumption values due to uncertainties in the determination of the azeotropic concentration as a function of pressure. For example, according to Black (2), the value for the low pressure limit—where the disappearance of the azeotrope occurs—is about 80 mmHg, while according to Collura and Luyben (3) this value is 36 mmHg, and according to Kolbe and Gmehling (4) it is 89 mmHg. In this work, this value is about 60 mmHg.

Black (2) compared several distillation schemes (atmospheric, vacuum, azeotropic, and extractive) for the production of anhydrous ethanol and gasohol. He concluded that the energy required for the ethanol recovery varies from 35 to 45% of the energy content of the ethanol depending on its purity and the type of process used. The most promising of the cases examined was the production of gasohol with azeotropic distillation using gasoline as an entrainer and consuming 34.6% of the energy content of ethanol for recovery.

Extensive results for a large number of distillation schemes have also been presented by Collura and Luyben (3). They reached an energy consumption of 5430 kJ/kg for a distillate 90 mol% in ethanol with a system of two distillation columns, operating at 1250 and 210 mmHg, respectively, which represents 18.5% of the energy content of pure ethanol. These values are very sensitive to distillate purity, and the energy consumption increases sharply when the concentration of ethanol in the distillate exceeds 90%.

These studies do not give details about the thermodynamic model used, but they give different azeotropic composition versus pressure curves. The energy consumption depends strongly on the thermodynamic model used. Our preliminary calculations, for example, suggest that a difference of about 1% in the prediction of the azeotropic composition at 220 mmHg leads to an increase of the energy consumption of about 50% when the desired purity of the product is close to this azeotropic composition. For reasonably accurate estimates of energy consumption, it is apparent that a reliable thermodynamic model is essential.

The possibility of ethanol recovery from aqueous solutions by supercritical fluid extraction has also been studied by many authors. Use of supercritical extraction with carbon dioxide is not considered effective by several authors [Brignole et al. (5, 6), Horizoe et al. (7)], while Paulaitis et al. (8, 9) suggest that carbon dioxide may be better at subcritical temperatures where three phases (liquid–liquid–gas) are formed. Use of propane as the supercritical solvent is postulated by Brignole and his coworkers based on phase equilibrium data obtained by prediction methods. The use of extractive distillation with propane at subcritical temperatures and high pressures (approximately 100 atm) is suggested by the pilot unit of Horizoe et al. (10), who also estimate a low energy consumption—1500 to 2500 kJ/kg of pure ethanol—from a feed of 10 wt% in ethanol. Their ensuing paper [Horizoe et al. (7)], however, suggests that some questions have to be answered. Finally, Hytoft et al. (11) presented energy consumption estimates for the separation of the water–ethanol system using supercritical propane, varying from 4600 to 5000 kJ/kg of pure ethanol from a feed of 49 wt% in ethanol. The great discrepancy in energy requirement estimates as well as the high capital cost, the complexity of the process simulation, and the lack of experience on the operation of such units at an industrial level has led to a limited number of present applications of the method.

In this study we present:

1. The water tolerance of gasoline–ethanol blends, which determines the purity of the bioethanol produced.
2. An analysis of the azeotropic concentration–pressure dependency based on the available literature for vapor–liquid equilibrium data of water–ethanol mixtures, as well as the development of a reliable Virial–Wilson model in order to determine the required operating pressure for the previously specified purity.
3. The results of an energy consumption analysis as a function of operating pressure and feed concentration for distillation processes using the developed model.
4. The sensitivity of energy requirements on the thermodynamic model used.
5. Two possible configurations of the separation unit, and an energy–cost analysis of each one.

THE WATER TOLERANCE OF GASOLINE–ETHANOL MIXTURES

Keller (1) presented an extensive study on the possibility of using alcohols as motor fuels. He concluded that four main parameters affect the water tolerance of gasoline–ethanol mixtures:

1. The ambient temperature

2. The ethanol concentration
3. The aromatic content of the gasoline
4. The presence of higher alcohols

Figures 1 and 2 present the effects of the first two parameters on water tolerance. From these figures, for a country with no extremely cold winters (minimum ambient temperature, −20°C; alcohol concentration in the mixture, 10 vol%; average aromatic content, 26% [Lygeros (12); and no higher alcohol content], the water tolerance of the fuel is 0.42 wt%.

Considering *d*(gasoline) = 0.74 g/cm^3 and *d*(ethanol) = 0.789 g/cm^3 at 20°C, the water content of ethanol is 4 wt% and, taking into account a safety factor of about 10%, the maximum allowable water content in the ethanol product for use as a fuel additive under these conditions is 3.5 wt%. Thus, the desirable purity of the product of the bioethanol recovery plant should be 96.5 wt% or 91.5 mol% in ethanol, which corresponds to 0.37 wt% of water in the gasoline. For a lower purity product, phase splitting may occur on cold days and two phases will be separated (an upper gasoline-rich phase and a lower ethanol-rich phase), causing highly

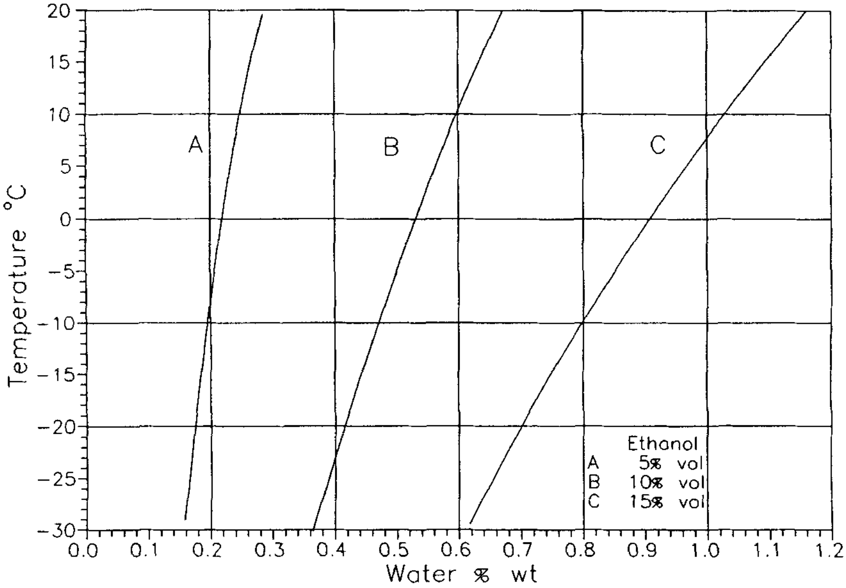

FIG. 1 Water tolerance of gasoline–ethanol blends as a function of the ethanol content (gasoline with 26% vol in aromatics).

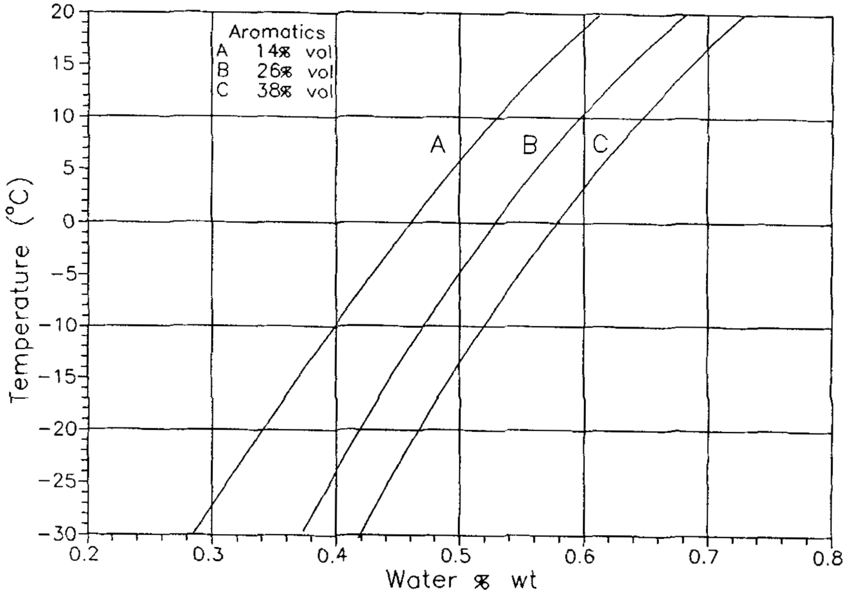

FIG. 2 The effect of aromatics on water tolerance (gasoline with 10% vol in ethanol).

undesirable effects. If the alcohol-rich phase picks up dirt or sediment, it can stall the engine when it reaches the carburetor, and it is highly corrosive to steel and to other metals parts of the engine. In addition, fuel in storage can lose some of its alcohol content, thus modifying the properties of the fuel and causing disposal problems at distribution and marketing facilities.

The results presented in these figures are further supported by the experimental measurements of Stephenson (13) at 25°C using a synthetic gasoline with a 34 vol% aromatics content, which suggests a solubility of 0.71 vs 0.76 through extrapolation of the data in Fig. 2. Therefore, the safety factor of 10% used for the calculation of the ethanol product purity also covers this deviation between the two sources.

Finally, Lojkasek et al. (14) indicated significant enhancement in water tolerance for gasoline–methanol mixtures in the presence of MTBE or other solubilizers. Their results are in good agreement with those of Keller. Since MTBE is often used as an antiknocking additive, the water content of the ethanol product could be greater, leading to more economical process designs.

THE THERMODYNAMIC MODEL

Data Base

The data base used to develop the thermodynamic model for the prediction of the VLE of ethanol–water mixtures as a function of the temperature is presented in Table 1. The systems with P–T–x–y data presented in Table 1 are those that were successfully tested with the method of Fredenslund et al. (25); those with P–T–x data were considered acceptable since no thermodynamic consistency test was possible.

The "experimental" azeotropic points were determined as follows. First the availability of each temperature's P–x data in the range $0.7 < x < 1.0$ were fitted with a polynomial $P = f(x)$ as shown for the case of 70°C in Fig. 3. The azeotropic points were then obtained by finding the x where P was maximum, and these numbers are presented in Table 1 and in graphical form in Fig. 4. The atmospheric pressure azeotropes reported by Kojima et al. (23), Gmehling (20), and Hrncirik (24) are also included. They represent the upper limit for the thermodynamic model to be developed.

The uncertainties observed with the azeotropic composition, shown in Figs. 3 and 4, are not surprising, considering the sensitivity of the x_{azeo}

TABLE 1
Experimental Azeotropic Points

No.	Type	T (°C)	P (mmHg)	x	Reference
1	T–P–x	30.0	78.6	0.9914	Pemberton et al. (15)
2	T–P–x–y	40.0	133.8	0.9540	Mertl (16)
3	T–P–x	50.0	221.4	0.9393	Balcazar-Ortiz et al. (17)
4	T–P–x	50.0	221.4	0.9370	Wilson et al. (18)
5	T–P–x	50.0	221.5	0.9360	Pemberton et al. (15)
6	T–P–x	50.0	221.9	0.9260	Chaudhry et al. (19)
7	T–P–x–y	55.0	280.6	0.9187	Mertl (16)
8	T–P–x–y	61.6	380.0	0.9058	Gmehling (20), System (1435) DDB
9	T–P–x	70.0	543.8	0.9081	Eftihidou (21)
10	T–P–x	70.0	544.1	0.9016	Rarey et al. (22)
11	T–P–x	70.0	544.7	0.8995	Pemberton et al. (15)
12	T–P–x	70.0	545.1	0.8950	Mertl (16)
13	T–P–x–y	78.2	760.0	0.8871	Gmehling (20), System (1028) DDB
14	T–P–x–y	78.2	760.0	0.8920	Kojima et al. (23)
15	T–P–x	78.2	760.0	0.8860	Hrncirik (24)

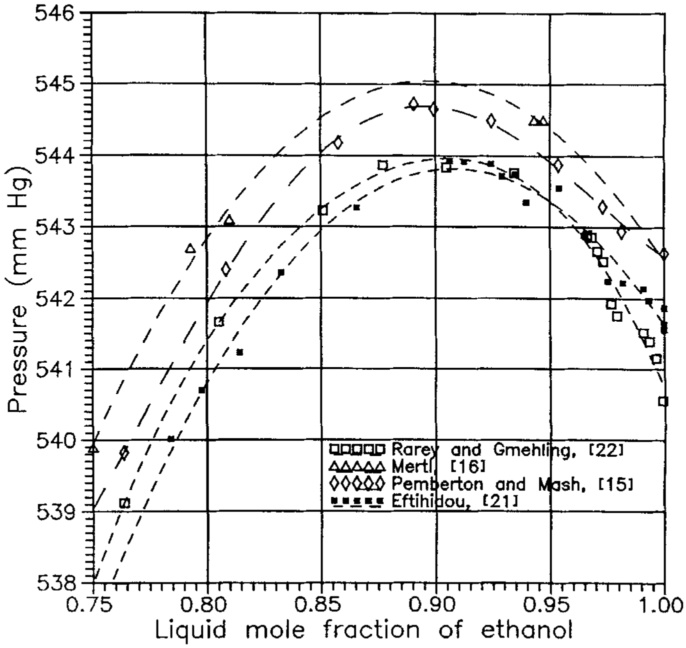

FIG. 3 P–x information for the water–ethanol system at 70°C.

to P as shown in Fig. 3; and the uncertainty in P measurements, also shown there, in terms of the reported P^s of the pure ethanol. Notice, for example, that for the azeotropic points of Fig. 3:

Rarey and Gmehling (22):	$x = 0.9016$ at 544.0 mmHg
Pemberton and Mash (15):	$x = 0.8995$ at 544.7 mmHg
Mertl (16):	$x = 0.8950$ at 545.1 mmHg
Eftihidou (21):	$x = 0.9081$ at 543.8 mmHg

the maximum deviation of P from the average of 544.4 mmHg, which equals 0.7 mmHg, is within the reported difference in P^s of pure ethanol. The VLE data of Eftihidou (21) for 70°C are given in Table 2.

Development of the Model

A thermodynamic model for the prediction of the vapor–liquid equilibrium of water–ethanol mixtures was developed as follows. For the de-

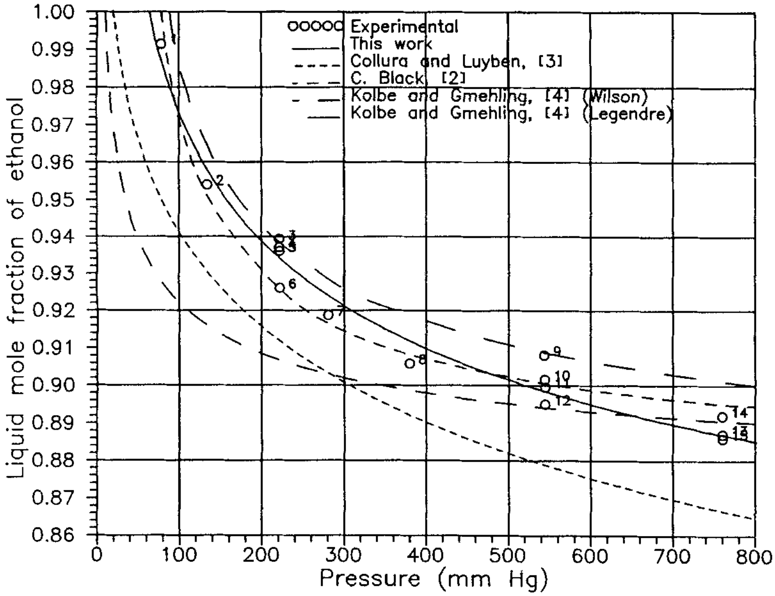

FIG. 4 Azeotropic composition as function of pressure. (The numbers by the symbols of the experimental points correspond to the ranking numbers of the data in Table 1.)

TABLE 2
Experimental VLE Data of Ethanol–Water at 70°C from Eftihidou (21)

P (mmHg)	*X*	*P* (mmHg)	*X*
541.87	1.0000	543.75	0.9348
541.64	1.0000	543.72	0.9289
541.56	1.0000	543.89	0.9243
541.98	0.9933	543.92	0.9126
542.15	0.9911	543.93	0.9063
542.23	0.9818	543.27	0.8657
542.25	0.9753	542.37	0.8326
542.89	0.9648	541.23	0.8143
543.56	0.9539	540.70	0.7977
543.35	0.9396	540.01	0.7841

scription of the vapor–liquid equilibrium:

$$\hat{f}_i^V = \hat{f}_i^l \tag{1}$$

the γ–ϕ approach was used [Tassios (26)]:

$$\hat{f}_i^V = y_i \hat{\phi}_i^V P \tag{2}$$

and

$$\hat{f}_i^l = x_i \gamma_i P_i^s \phi_i^s \exp\left(\frac{V_i(P - P_i^s)}{RT}\right) \tag{3}$$

where ϕ_i^V is the vapor-phase fugacity coefficient x_i, y_i is the molar composition of liquid and vapor phase, respectively
γ_i is the activity coefficient
P_i^s is the vapor pressure of pure i at the system temperature T
ϕ_i^s is the fugacity coefficient of saturated pure liquid i at T
V_i is the molar volume of pure liquid i at T

The exponential term expresses the Poynting effect (Pe).

For the prediction of the fugacity coefficients, the Virial Equation of State was used. The second virial coefficient was obtained by Tsonopoulos (27) correlations. Since a and b values for water, proposed by Tsonopoulos, where obtained for $T > 150°C$, we reestimated these values for water and ethanol, using the proposed values of B_{ii} by Kolbe and Gmehling (4). In order to be in absolute agreement with Kolbe and Gmehling, we also recalculated the value of k_{ij} using the cross coefficient B_{ij} proposed by them. Thus, the values for the Tsonopoulos correlations are

$$\alpha_{H_2O} = -0.01404, \qquad a_{EtOH} = 0.14259$$

$$b_{H_2O} = -0.00137, \qquad b_{EtOH} = 0.07991$$

$$k_{ij} = 0.04956$$

For the calculations of the liquid volume, the following equation, given by Daubert and Danner (28), was used:

$$d = \frac{A}{B^{[1+(1-T_r)^C]}} \tag{4}$$

where T_r is the reduced temperature and d is the liquid density in kmol/m^3. The coefficients used are presented in Table 3.

Vapor pressures of the pure components were predicted with the Antoine equation by using the coefficients values given by Gmehling et al. (29). Activity coefficients were expressed as a function of concentration

TABLE 3
Coefficients for Eq. (4)

Compound	*A*	*B*	*C*
Ethanol	1.648	0.27627	0.2331
Water	5.459	0.30542	0.0810

through the Wilson equation [Tassios (26)], and considering the temperature range involved, linearly *T*-dependent parameters were used.

The coefficients of the temperature dependency of the Wilson parameters were calculated through a regression procedure, using the following minimization function. This minimization function considers the average absolute percentage deviation between calculated and experimental pressure ($\%\Delta P$) and vapor concentration ($\Delta y \times 1000$) (if available) for each data set, along with the absolute percent deviation for the azeotropic pressure ($\%\Delta P_{az}$) and the azeotropic composition ($\%\Delta x_{azeo} \times 1000$) in this set. This minimization function is shown in Eq. (5):

$$\sum_{i=1}^{NS} \left\{ \%\Delta P_{azeo} + \Delta x_{azeo} \times 1000)_i^2 + \left(\frac{\sum_j^{ND} (\%\Delta P_j + \Delta y_j \times 1000)}{ND} \right)_i^2 \right\} \quad (5)$$

where *NS* is the numbers of the data sets and *ND* the number of the VLE data points for each set.

This minimization function gives emphasis on the description of the azeotropic point without sacrificing the corresponding VLE data. The resulting temperature-dependent equations are the following:

$$\Delta\lambda_{12} = 1778.51 - 4.3087T \quad (6)$$

$$\Delta\lambda_{21} = -759.59 + 4.9626T \quad (7)$$

with T in K and $\Delta\lambda_{ij}$ in cal/mol.

Results and Comparisons

The proposed model describes the VLE data sets with average absolute percent deviation in pressure $\%\Delta P\% = 1.1$ (maximum 2.3%) and average deviation in vapor concentration $\Delta y \times 1000 = 5.3$ (maximum 7.5), while the predicted azeotropic points, presented in Fig. 4, are in good agreement with the "experimental" ones, considering the uncertainty of the latter. It also predicts the disappearance of the azeotrope at 60 mmHg, about halfway between Black's and Collura's predictions.

With reference to Fig. 3, the proposed model predicts an azeotropic point at 70°C of $P = 546.3$ mmHg and $x = 0.897$, well within the uncertainty of the experimental data presented there.

Figure 4 also presents the results of the models proposed by Collura and Luyben (3) and by Black (2) as taken from the corresponding figures of their publications, and of Kolbe and Gmehling (4). The Collura and Luyben model consistently underestimates the azeotropic points, including the rather accurately known atmospheric one, while that of Black is in much better agreement with them.

Kolbe and Gmehling (4), in order to describe the VLE data, as well as the excess properties of the ethanol/water system, proposed a Legendre polynomial for the excess Gibbs energy which resulted in a temperature-dependent model with 24 parameters, obtained by fitting VLE data in the range of 30–150°C. The second virial coefficients, used by Kolbe and Gmehling, have also been obtained by fitting experimental values. They also used a Wilson model to correlate the VLE behavior of this system with temperature-dependent parameters (second degree polynomial). The VLE behavior of these models (Legendre and Wilson) is similar to the behavior of the proposed one. However, by using the Wilson model, proposed by Kolbe and Gmehling, the description of the experimental azeotropic points is not satisfactory at low pressures (Fig. 4). On the other hand, their Legendre model performs well in the description of the azeotropic points for a large temperature range, as can be seen in the corresponding figure of their publications, but in the pressure range studied in this work, the proposed model performs better than this model does (Fig. 4). This Legendre model also predicts the c_p^E and h^E values of the system better than the Wilson ones, but these values are of limited importance considering that, e.g., the value of h^E at 70°C never exceeds the 200 J/mol of the mixture when the enthalpy of vaporization has values greater than 40,000 J/mol.

Therefore, the model proposed in this work is a simple but reliable Wilson model that can accurately predict both the VLE behavior and the azeotropic concentrations. This model will be used in the distillation calculations that follow.

THE ENERGY CONSUMPTION FOR ETHANOL RECOVERY

In this section we report the effect of the feed concentration and the pressure on the energy requirements, and in the next section the effect of the uncertainty in the azeotropic composition on the same; we then present an energy–cost analysis for two possible separation scheme. For this purpose, the following design parameters were used with the objective of obtaining a distillate product of 91.5 mol% (96.5 wt%) in ethanol as determined by the analysis of water tolerance for the fuel blends. The recovery of ethanol was 99.5% of the feed ethanol content. The feed was preheated by the bottoms product and inserted in the column at its bubble point temperature at the column operating pressure. If additional heat was required, it could have been supplied either with preheating through the distillate cooler, or through a steam heater. The pressure is assumed constant throughout the column. The Naphthali–Sandholm algorithm was used for simulation of the column. Feed and cooling waters were available at 25°C, and a temperature difference of 10°C was set between the streams of the heat exchanger.

The effect of feed concentration on energy demand, shown in Fig. 5 for two different pressure levels, is not significant, at least not for the 7 wt% level used here, that leads to high efficiencies in the enzymatic reactions for the production of bioethanol [Macris (30)]. The effect becomes somewhat more significant for lower concentrations.

Figure 4 indicates that, according to the proposed model, it is theoretically possible to recover the desired 91.5 mol% ethanol-rich product for

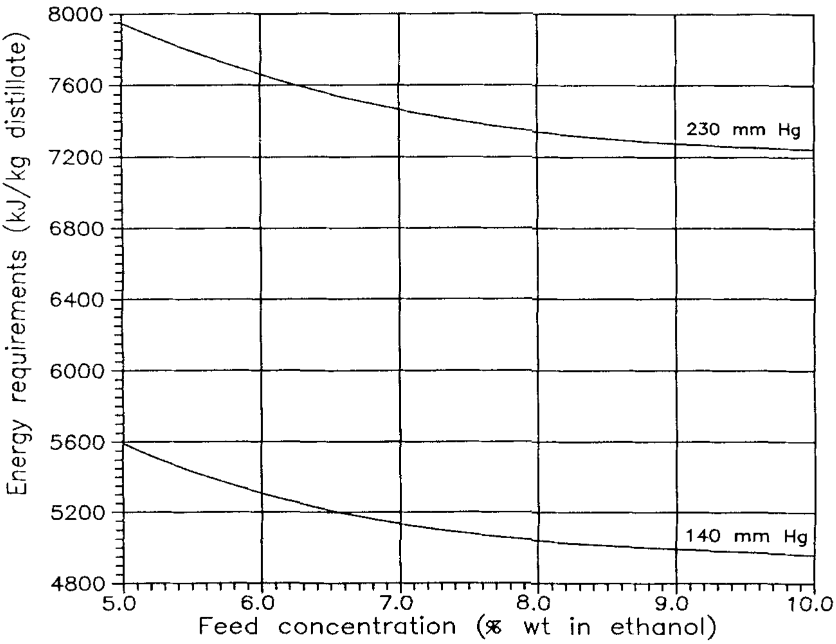

FIG. 5 Feed concentration influences on energy requirements. (Number of stages, 40; distillate, 91.5% ethanol; recovery, 99.5%.)

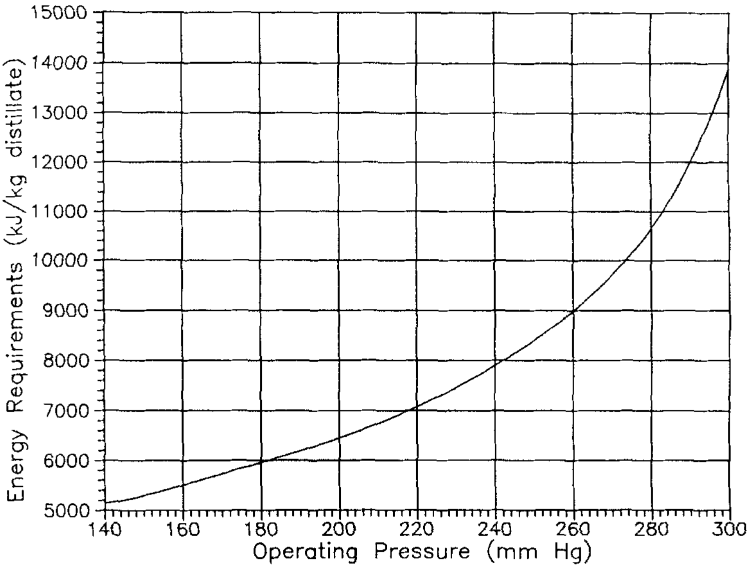

FIG. 6 Operating pressure influence on energy demand. (Number of stages, 40; feed concentration, 7% wt in ethanol; distillate, 91.5% ethanol; recovery, 99.5%.)

a pressure of 340 mmHg. Of course, this could be only obtained by a distillation column with an infinite number of trays. Therefore, operating pressures of less than 280 mmHg should be used.

The effect of pressure on the energy requirements is shown in Fig. 6. A significant increase of energy demand is observed with increasing pressure. Pressures less than 140 mmHg are not recommended because the temperature in the distillate condenser drops below the 35°C limit for cooling water use and the cost increases sharply due to the need for a refrigeration unit. Thus, operating pressures of about 140–150 mmHg are the most desirable.

THE SENSITIVITY OF THE ENERGY REQUIREMENTS ON THE THERMODYNAMIC MODEL USED

Considering the uncertainty in azeotropic composition, as demonstrated in Fig. 4, its impact on the energy requirement for a given ethanol–water separation was then examined. For this purpose we modified the constant in Eq. (7) for the Wilson parameter $\Delta\lambda_{21}$ from -759.6 to -749.6. The resulting azeotropic composition vs pressure curve—referred to as "modified"—is shown, along with the "original" one and the corresponding energy consumptions, in Fig. 7. This modification leads to an almost parallel transposition of the curve to lower compositions, resulting to higher energy requirements. Thus, at 160 mmHg (where the azeotropic composition is much greater than the desirable one—91.5%—for both models), the use of the modified model leads to an increase of 18%, while at 220 mmHg (where the azeotropic composition for the modified model is close to the desirable one) it leads to a 47% increase of energy consumption. Apparently the use of a reliable model is very important, especially if a scheme operates in the near-azeotropic region, because small deviations in the thermodynamic behavior can lead to significant ones in the predicted energy consumption.

This sensitivity explains the difference between calculations performed by Collura and ones performed by us. For a standard column design, 210 mmHg operating pressure and 90% distillate product, Collura suggests 6315 kJ/kg of product. Our calculations, for exactly the same scheme, suggest 4770 kJ/kg, which is a 24% difference from Collura's.

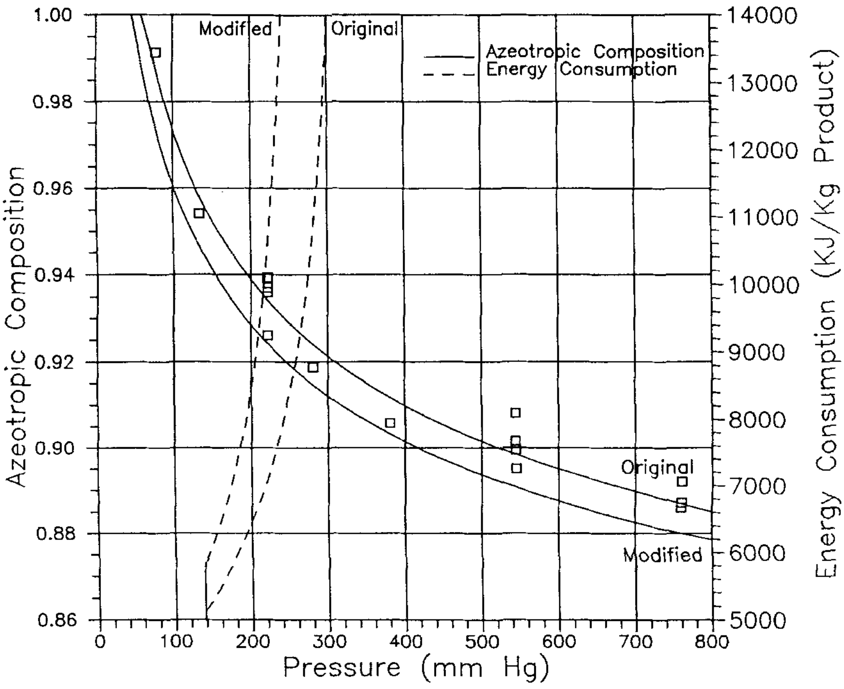

FIG. 7 Sensitivity analysis of the thermodynamic model results.

These differences are justified by the difference in the description of the azeotropic line. As can be observed in Fig. 4, the expected purity (90%) is next to the azeotropic region for Collura's model. On the other hand, this purity is not as close to the azeotropic line for our model. Collura's line differs by 0.03 in x_{azeo} at low pressures and 0.02 at atmospheric pressures, while the uncertainty of the experimental points demonstrated is only 0.01.

THE ENERGY–COST ANALYSIS OF TWO ALTERNATIVE SEPARATION PROCESS CONFIGURATIONS

Two alternative process configurations were examined and compared on an energy consumption versus total annual cost basis. The first one, Fig. 8, contains a single distillation column, while the second one, Fig. 9, contains two distillation columns thermally integrated. Although the mechanical recompression scheme, examined by Collura, decreases the annual cost (14%) (decrease in operational cost by energy saving), it is not studied in this work because of the large increase of the capital cost (55%).

The unit is designed for 1000 kmol/h of 91.5% ethanol. The feed ethanol concentration is set to 7 wt%, a typical one for enzymatic reactions; the distillate ethanol concentration to 96.5 wt% (91.5 mol%) and the recovery of ethanol to 99.5% for each column.

To thermally integrate the distillation units, the feed is preheated by the distillate and the bottoms of each unit. Also, for the second configuration the operating pressure levels of the columns are properly defined so that the condenser of the high pressure one (prefractionator) can be used as the boiler of the low pressure one. The Murphee efficiencies used for the calculation of the actual plate number from the number of (equilibrium) stages are 40% for the stripping and 50% for the rectification section of the columns.

For cost estimation, the following assumptions have been made:

1. The capital cost is calculated through the correlations given by Guthrie (31), updated to mid-1993.
2. The operating cost is calculated by adding the electricity, cooling water, and heating steam costs over a year period.
3. For the total annual cost estimation—fixed, operating, and maintenance—a 10-year depreciation time of the capital cost is used for the fixed cost calculation, and 1.7% of the fixed cost is used for calculation of the annual maintenance cost.

As far as the cost estimation is concerned, there is great uncertainty in the final numbers. This is because modifications in the assumptions made

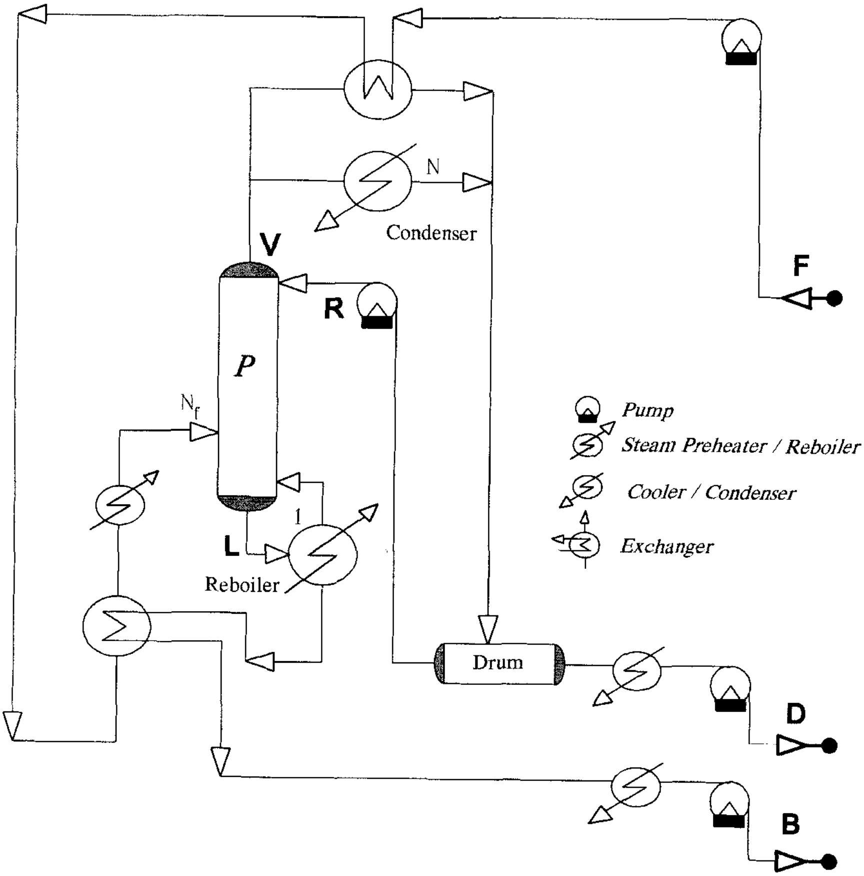

FIG. 8 Single column configuration (SCC).

by the authors can significantly change the money amounts. However, the dependency of cost on the possible energy saving can be observed by the cost estimation performed here.

For the single column configuration, the energy requirements and the annual cost are as shown in Fig. 10 at different operating pressures and number of stages values. Low pressures and a high number of stages lead to both lower energy requirements and costs. An operating pressure of 140 mmHg and a 40-stage column seems to be the most preferable combination and leads to a 5150 kJ/kg of product energy consumption with a total cost of 7.92 millions US$/year. Numbers of (equilibrium) stages

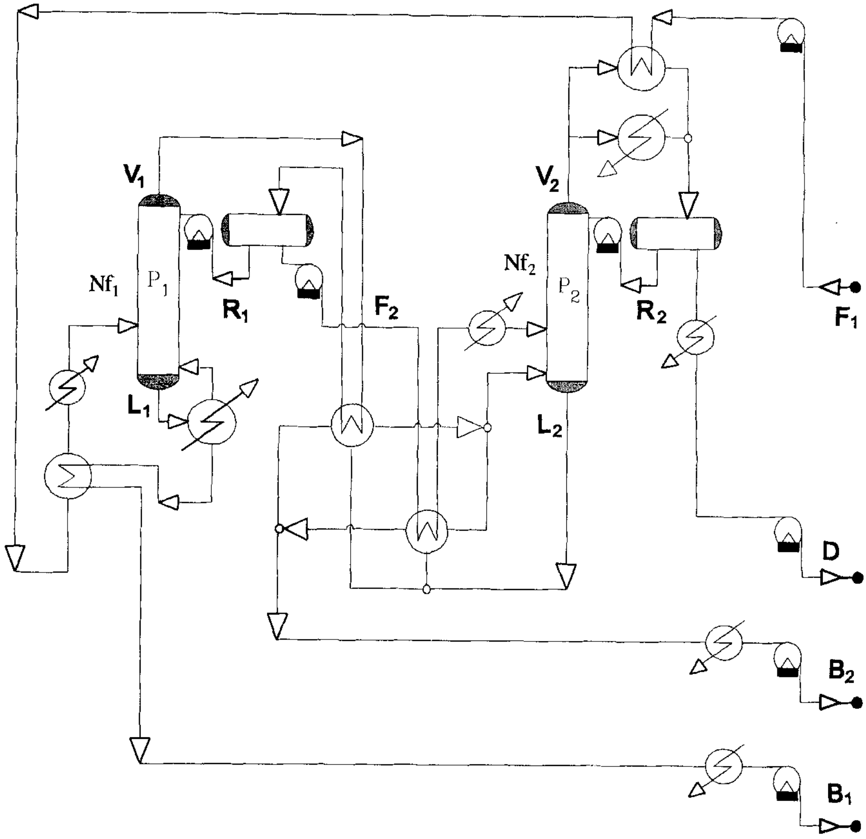

FIG. 9 Two thermally integrated columns configuration (TICC).

greater than 45 are not recommended because they lead to actual plate numbers greater than 100 and thus to unrealistic high columns.

For the two-column configuration, the intermediate product composition—distillate of the high pressure column (1st column) and feed to the low pressure one (2nd column)—is an additional very important optimization parameter besides the operating pressure levels and the number of stages of the columns.

Table 4 presents typical results of the developed process simulator for the two-column configuration. The effects of the operating pressures and the number of stages of each column on the energy requirements and the total annual cost are considered for four intermediate concentration levels.

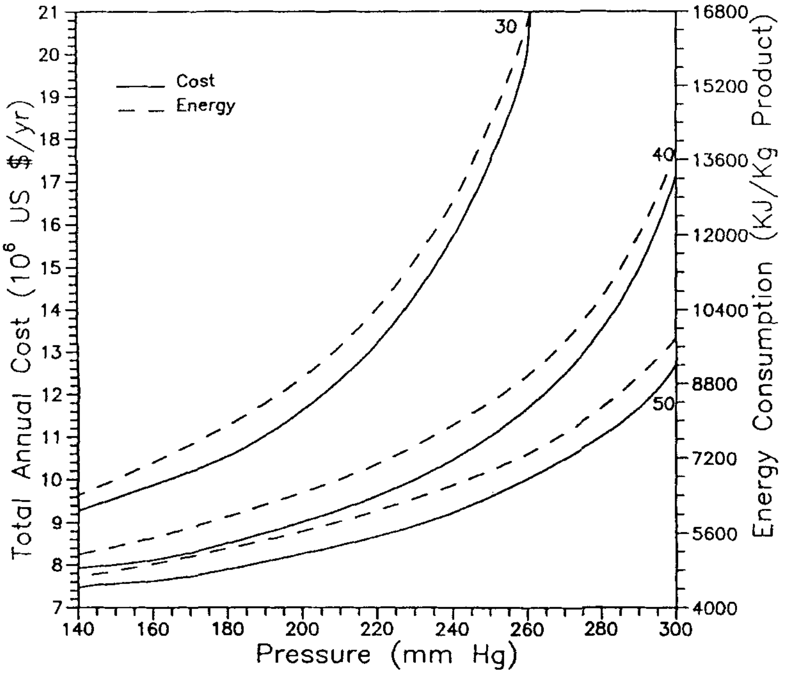

FIG. 10 Energy requirements and annual cost as a function of the operating pressure and number of stages values.

These results are compared to those of the single column configuration. The percentage deviations of the energy and cost are also presented in Table 4.

The operating pressure of the second column was set to 140 mmHg and the number of stages was always kept less than 40 because, according to observations on the operation of the single column, these values lead to minimum energy consumption for a reasonable column height. The operating pressure and the number of stages for the first column were calculated by assuming that the heat load rejected by the condenser of this column should be equal to the one needed in the reboiler of the second one, and at temperatures suitable for this heat exchange. Of course, these values also depend on the distillate concentration in ethanol.

The operation of the first column at pressures slightly over atmospheric with intermediate concentrations of 85–86% in ethanol leads to about a 13% decrease of the energy requirements with about a 13% increase of the total annual cost. On the other hand, its operation at subatmospheric

TABLE 4
Energy Consumption and Total Annual Cost of Various Separation Unit Configurations

P_1 (mmHg)	N_1	Xd_1 (%mol)	P_2 (mmHg)	N_2	Energy consumption (kJ/kg)	% Decrease over single column	Total cost (MUS $/year)	% Increase over single column
Single column configuration			140	40	5147		7.92	
810	34	85	140	40	4518	12.2	9.01	13.7
605	30	85	140	40	4495	12.7	9.00	13.6
500	28	85	140	40	4483	12.9	9.11	15.0
770	40	86	140	40	4449	13.6	8.94	12.8
700	40	86	140	40	4376	15.0	8.91	12.4
485	40	86	140	40	4352	15.5	8.98	13.3
405	40	87	140	40	4143	19.5	8.86	11.8
315	35	87	140	40	4137	19.6	9.11	15.0
280	40	88	140	32	4103	20.3	9.03	14.0

conditions results in an almost 20% decrease of energy load at the same cost increase.

CONCLUSIONS

An extensive study of the possibility of obtaining near-anhydrous ethanol as a gasoline additive resulted in a desirable concentration of the product in ethanol and to the development of a simple, but accurate, Wilson–Virial thermodynamic model for the prediction of the VLE of the ethanol–water system.

The development of this new model was necessary because:

The prediction of energy consumption from process simulation is very sensitive to small deviations in VLE behavior in the near-azeotropic region.

There is significant uncertainty in the existing models and in the "experimental" azeotropic data.

Our model was used in a computer simulator of a distillation unit, and the energy requirements along with the total annual cost were calculated for two possible configurations of the separation unit.

For the single column configuration, the energy requirements are about 5.2 MJ/kg of product and, considering an energy content of 29.7 MJ/kg (23.5 MJ/L in 20°C) for the ethanol, the energy consumption for the recovery of a product 96.5 wt% in ethanol rises to 17.5% of the energy content of pure ethanol. A thermally integrated sequence of two distillation columns provides a 13% saving of the required energy with a 13% increase of the total annual cost. Thus, there are more than 25 MJ/kg available to cover all the other energy demands of production: cultivation, fermentation, drying of by-products, transportation, etc.

The final feasibility analysis and decision making on the configuration of the separation unit should also take into account such ecological and political factors as reduction of dependence of the country on foreign energy sources, currency savings, etc.

ACKNOWLEDGMENT

We would like to thank the Centre of Renewable Energy Sources (C.R.E.S) for its financial support of this work.

REFERENCES

1. K. L. Keller, "Alcohols as Motor Fuel?," *Hydrocarbon Processing*, *59*(5), 127–138 (1979).
2. C. Black, "Distillation Modelling of Ethanol Recovery and Dehydration Processes for Ethanol and Gasohol," *Chem. Eng. Prog.*, *76*(9), 78–85 (1980).
3. M. A. Collura and W. L. Luyben, "Energy-Saving Distillation Designs in Ethanol Production," *Ind. Eng. Chem. Res.*, *27*, 1686–1696 (1988).
4. B. Kolbe and J. Gmehling, "Thermodynamic Properties of Ethanol + Water. II. Potentials and Limits of G^E Models," *Fluid Phase Equil.*, *23*, 227–241 (1985).
5. E. A. Brignole, S. Skjold-Jorgensen, and Aa. Fredenslund, "Application of a Local Composition Equation of State to Supercritical Fluid Phase Equilibrium Problems," *Ber. Bunsenges. Phys. Chem.*, *88*, 801–806 (1984).
6. E. A. Brignole, P. M. Andersen, and Aa. Fredenslund, "Supercritical Fluid Extraction of Alcohols from Water," *Ind. Eng. Chem. Res.*, *26*, 254–261 (1987).
7. H. Horizoe, T. Tanimoto, I. Yamamoto, and Y. Kano, "Phase Equilibrium Study for the Separation of Ethanol–Water Solution Using Subcritical and Supercritical Hydrocarbon Solvent Extraction," *Fluid Phase Equil.*, *84*, 297–320 (1993).
8. M. E. Paulaitis, M. L. Gilbert, and C. A. Nash, *Separation of Ethanol–Water Mixtures with Supercritical Fluids*, Paper Presented at the 2nd World Congress of Chemical Engineering, Montreal, Canada, October 5, 1981.
9. M. E. Paulaitis, R. G. Kander, and J. R. DiAndreth, "Phase Equilibria Related to Supercritical-Fluid Solvent Extractions," *Ber. Bunsenges. Phys. Chem.*, *88*, 869–875 (1984).
10. H. Horizoe, T. Tanimoto, I. Yamamoto, K. Ogawa, Y. Kano, and M. Maki, *Supercritical Fluid Extraction of Ethanol from Water Using Hydrocarbon Solvent*, Paper Presented at 2nd International Symposium on Supercritical Fluids, Boston, Massachusetts, May 20–22, 1991.
11. G. Hytoft, R. Gani, and Aa. Fredenslund, "Design and Analysis of Supercritical Ex-

traction Processes," in *Energy Efficiency in Process Technology* (P. A. Pilavachi, Ed.), Elsevier Applied Science, 1993, pp. 398–411.

12. A. Lygeros, Hellenic Aspropyrgos Refinery, Athens, Greece. Personal Communication, 1992.
13. R. M. Stephenson, "Mutual Solubilities: Water–Ketones, Water–Ethers, and Water–Gasoline–Alcohols," *J. Chem. Eng. Data*, *37*(1), 80–95 (1992).
14. M. Lojkasek, V. Ruzicka Jr., and A. Kohoutova, "Solubility of Water in Blends of Gasoline, Methanol and a Solubilizer," *Fluid Phase Equil.*, *71*(1–2), 113–123 (1992).
15. R. C. Pemberton and C. J. Mash, *J. Chem. Thermodyn.*, *10*, 867 (1978).
16. I. Mertl, *Collect. Czech. Chem. Commun.*, *37*, 336 (1972).
17. A. M. Balcazar-Ortiz, R. B. Patel, M. M. Abbott, and H. C. Van Ness, *J. Chem. Eng. Data*, *24*, 133 (1979).
18. S. R. Wilson, R. B. Patel, M. M. Abbott, and H. C. Van Ness, *Ibid.*, *24*, 130 (1979).
19. M. M. Chaudhry, H. C. Van Ness, and M. M. Abbott, *Ibid.*, *25*, 254 (1979).
20. J. Gmehling, *Dortmund Data Bank*, *Software Development in Chemistry*, 5th ed., Springer, Berlin, 1991.
21. E. Eftihidou, "VLE Measurements of Ethanol–Water Mixtures." M.S. Thesis, NTUA, 1993.
22. J. R. Rarey and J. Gmehling, "Computer-Operated Differential Static Apparatus for the Measurement of Vapor–Liquid Equilibrium Data," *Fluid Phase Equil.* *83*, 279–287 (1993).
23. K. Kojima, K. Tochigi, H. Seki, and K. Watase, *Kagaku Kogaku*, *32*, 149 (1968).
24. F. Hrncirik, *Chem. Prum.*, *29*, 539 (1979).
25. Aa. Fredenslund, J. Gmehling, and P. Rasmussen, *Vapor–Liquid Equilibria Using UNIFAC: A Group Contribution Method*, Elsevier Scientific Publishing, 1977, p. 68.
26. D. Tassios, *Chemical Engineering Thermodynamics*, Springer-Verlag, 1993.
27. C. Tsonopoulos, "An Empirical Correlation of Second Virial Coefficients," *AIChE J.*, *20*(2), 263–272 (1974).
28. T. E. Daubert and R. P. Danner, *Data Compilation Tables of Properties of Pure Compounds*, AIChE/DIPPR Data, 1985, 1989.
29. J. Gmehling, U. Onken, and W. Arlt, *Vapor–Liquid Equilibrium Data Collection, Dechema, Chemistry Data Series*, Vol. I, Part 1a, 1981.
30. V. Macris, Laboratory of Biochemical Engineering, NTU, Athens, Greece, Personal Communication, 1993.
31. K. M. Guthrie, "Data and Techniques for Preliminary Capital Cost Estimating," *Chem. Eng.*, *24*, 114–142 (1969).

Received by editor August 1, 1994